A Spectral Method for Parabolic Differential Equations

Kendall Atkinson
Departments of Mathematics & Computer Science
The University of Iowa

Olaf Hansen
Department of Mathematics
California State University - San Marcos

David Chien
Department of Mathematics
California State University - San Marcos

June 28, 2012

Abstract

We present a spectral method for parabolic partial differential equations with zero Dirichlet boundary conditions. The region Ω for the problem is assumed to be simply-connected and bounded, and its boundary is assumed to be a smooth surface. An error analysis is given, showing that spectral convergence is obtained for sufficiently smooth solution functions. Numerical examples are given in both $\mathbb{R}^2$ and $\mathbb{R}^3$.

1 INTRODUCTION

Consider solving the parabolic partial differential equation

$$\frac{\partial u\,(s,t)}{\partial t} = \sum_{k,\ell=1}^{d} \frac{\partial}{\partial s_k}\left(a_{k,\ell}(s,t,u\,(s,t))\frac{\partial u(s,t)}{\partial s_\ell}\right) + f\,(s,t,u\,(s,t))\,, \tag{1}$$

for $s \in \Omega \subseteq \mathbb{R}^d$, $0 < t \leq T$. The solution u is subject to the Dirichlet boundary condition

$$u(s,t) \equiv 0, \qquad s \in \partial\Omega, \quad 0 < t \leq T \tag{2}$$

and to the initial condition

$$u\,(s,0) = u_0\,(s)\,, \qquad s \in \Omega. \tag{3}$$

The region Ω is open, bounded, and simply connected in $\mathbb{R}^d$ for some $d \geq 2$, and the boundary $\partial\Omega$ is assumed to be several times continuously differentiable. This paper presents a spectral method for solving this problem. The functions $a_{i,j}(s,t,z)$ and $f(s,t,z)$ are assumed to be continuous for $(s,t,z) \in \overline{\Omega} \times [0,T] \times \mathbb{R}$. Additional assumptions are given later in the paper. These assumptions are stronger than needed for the results we obtain, but they simplify the presentation. In addition, we assume that there is a unique solution u to the problem (1)-(3). Later in §2.3 we address the problem of handling a nonhomogeneous boundary condition, extending (2). For an introduction to the theory of nonlinear parabolic problems using variational methods, see [28, Chap. 30].

We transform the above problem to one over the unit ball $\mathbb{B}_d$ in $\mathbb{R}^d$, and then we use Galerkin's method with a suitably chosen polynomial basis to approximate the solution u. This is similar in spirit to earlier work in [2], [5], [7]. This approach reduces the problem to the solution of an inital value problem for a system of ordinary differential equations, for which there is much excellent software. The convergence analysis of the paper depends on the landmark paper of Douglas and Dupont [13]. The methods of this paper also extend to having the functions $a_{i,j}$ and f depend on the first derivatives $\partial u/\partial s_j$, although this is not considered here. For related books on spectral methods for partial differential equations, see [10]-[12], [16], [17], [23], [24].

The spectral method is presented and analyzed in §2, implementation issues are discussed in §3, and numerical examples in $\mathbb{R}^2$ and $\mathbb{R}^3$ are given in §4.

2 A spectral method

We transform the problem (1)-(3) to one over the unit ball $\mathbb{B}_d$, and then we apply Galerkin's method using multivariate polynomials as approximations of the solution. To transform a problem defined on Ω to an equivalent problem defined on $\mathbb{B}_d$, we review some ideas from [2] and [7], modifying them as appropriate for this paper.

Assume the existence of a function

$$\Phi : \overline{\mathbb{B}}_d \underset{onto}{\overset{1-1}{\longrightarrow}} \overline{\Omega} \tag{4}$$

with Φ a twice–differentiable mapping, and let $\Psi = \Phi^{-1} : \overline{\Omega} \underset{onto}{\overset{1-1}{\longrightarrow}} \overline{\mathbb{B}}_d$. For $v \in L^2(\Omega)$, let

$$\widetilde{v}(x) = v(\Phi(x)), \qquad x \in \overline{\mathbb{B}}_d \subseteq \mathbb{R}^d \tag{5}$$

and conversely,

$$v(s) = \widetilde{v}(\Psi(s)), \qquad s \in \overline{\Omega} \subseteq \mathbb{R}^d. \tag{6}$$

Assuming $v \in H^1(\Omega)$, we can show

$$\nabla_x \widetilde{v}(x) = J(x)^{\mathrm{T}} \nabla_s v(s), \qquad s = \Phi(x)$$

with $J(x)$ the Jacobian matrix for Φ over the unit ball $\mathbb{B}_d$,

$$J(x) \equiv (D\Phi)(x) = \left[\frac{\partial \varphi_i(x)}{\partial x_j}\right]_{i,j=1}^{d}, \qquad x \in \overline{\mathbb{B}}_d. \tag{7}$$

To use our method for problems over a region Ω, it is necessary to know explicitly the functions Φ and J. We assume

$$\det J(x) \neq 0, \qquad x \in \overline{\mathbb{B}}_d. \tag{8}$$

Similarly,

$$\nabla_s v(s) = K(s)^{\mathrm{T}} \nabla_x \widetilde{v}(x), \qquad x = \Psi(s)$$

with $K(s)$ the Jacobian matrix for Ψ over Ω. By differentiating the identity

$$\Psi(\Phi(x)) = x, \qquad x \in \overline{\mathbb{B}}_d$$

we obtain

$$K(\Phi(x)) = J(x)^{-1}.$$

Assumptions about the differentiability of $\widetilde{v}(x)$ can be related back to assumptions on the differentiability of $v(s)$ and $\Phi(x)$.

Lemma 1 *If $\Phi \in C^m\left(\overline{\mathbb{B}}_d\right)$ and $v \in C^k\left(\overline{\Omega}\right)$, then $\widetilde{v} \in C^q\left(\overline{\mathbb{B}}_d\right)$ with $q = \min\{k, m\}$.*

Proof. A proof is straightforward using (5). ∎

A converse statement can be made as regards $\widetilde{v}$, v, and Ψ in (6).

Often a mapping φ is given from $\mathbb{S}^{d-1}$ onto $\partial\Omega$, and it will not be clear as to how to extend the mapping to Φ satisfying (4) and (8). This is explored in [6] with several methods given for constructing Φ.

To obtain a space for approximating the solution u of our problem, we proceed as follows. Denote by Π_n the space of polynomials in d variables that are of degree $\leq n$: $p \in \Pi_n$ if it has the form

$$p(x) = \sum_{|i| \leq n} a_i x_1^{i_1} x_2^{i_2} \dots x_d^{i_d}$$

with i a multi–integer, $i = (i_1, \dots, i_d)$, and $|i| = i_1 + \cdots + i_d$. Our approximation space with respect to $\mathbb{B}_d$ is

$$\widetilde{\mathcal{X}}_n = \left\{ \left(1 - |x|^2\right) p(x) \mid p \in \Pi_n \right\} \subseteq H_0^1(\mathbb{B}_d) \tag{9}$$

With respect to Ω, the approximating subspace is

$$\mathcal{X}_n = \left\{ \psi(s) = \widetilde{\psi}(\Psi(s)) : \widetilde{\psi} \in \widetilde{\mathcal{X}}_n \right\} \subseteq H_0^1(\Omega) \tag{10}$$

Let $N_n = \dim \mathcal{X}_n = \dim \widetilde{\mathcal{X}}_n = \dim \Pi_n$. For $d = 2$, $N_n = (n+1)(n+2)/2$.

2.1 The approximation

We reformulate the parabolic problem (1)-(3) as a variational problem. Multiply (1) by an arbitrarily chosen $v \in H_0^1(\Omega)$ and perform integration by parts, obtaining

$$\begin{aligned}\left(\frac{\partial u(\cdot,t)}{\partial t}, v\right) = &-\sum_{i,j=1}^{d}\int_\Omega a_{i,j}(s,t,u(s,t))\frac{\partial u(s,t)}{\partial s_i}\frac{\partial v(s,t)}{\partial s_j}\,ds \\ &+(f(\cdot,t,u(\cdot,t)),v), \qquad v\in H_0^1(\Omega), \quad t\geq 0.\end{aligned} \tag{11}$$

In this equation, $(\cdot,\cdot)$ denotes the usual inner product for $L^2(\Omega)$. Equation (11), together with (3), is used to develop our approximation method.

We look for a solution of the form

$$u_n(s,t) = \sum_{k=1}^{N_n}\alpha_k(t)\psi_k(s) \tag{12}$$

with $\{\psi_1,\ldots,\psi_N\}$ a basis of $\mathcal{X}_n$. The coefficients $\{\alpha_1,\ldots,\alpha_{N_n}\}$ generally will vary with n, but we omit the explicit dependence to simplify notation. Substitute this u_n into (11) and let v run through the basis elements ψ_ℓ. This results in the following system:

$$\begin{aligned}&\sum_{k=1}^{N_n}\alpha_k'(t)(\psi_k,\psi_\ell) \\ &\quad=-\sum_{k=1}^{N_n}\alpha_k(t)\sum_{i,j=1}^{d}\int_\Omega a_{i,j}\left(s,t,\sum_{k=1}^{N_n}\alpha_k(t)\psi_k(s)\right)\frac{\partial\psi_k(s,t)}{\partial s_i}\frac{\partial\psi_\ell(s,t)}{\partial s_j}\,ds \\ &\qquad+\left(f\left(\cdot,t,\sum_{k=1}^{N_n}\alpha_k(t)\psi_k\right),\psi_\ell\right), \quad \ell=1,\ldots,N_n, \quad t\geq 0\end{aligned} \tag{13}$$

This is a system of ordinary differential equations for the coefficients α_k, for $k=1,\ldots,N_n$. For the initial conditions, calculate

$$u_0(s)\approx u_{0,n}(s)\equiv\sum_{k=1}^{N_n}\alpha_k^{(0)}\psi_k(s) \tag{14}$$

by some means, and then use

$$\alpha_k(0)=\alpha_k^{(0)}, \qquad k=1,\ldots,N_n. \tag{15}$$

The implementation of (12)-(15) is discussed in §3.

2.2 Convergence analysis

Our error analysis of (12)-(15) is based on Douglas and Dupont [13, Thm. 7.1]; and as in that paper, we assume the functions $\{a_{i,j}\}$ and f satisfy a number of properties.

A1 As stated earlier, we assume the functions $a_{i,j}(s,t,z)$ and $f(s,t,z)$ are continuous for $(s,t,z) \in \overline{\Omega} \times [0,T] \times \mathbb{R}$. Moreover, assume

$$|f(s,t,r) - f(s,t,\rho)| \leq K|r-\rho|,$$

for all $(s,t,r),(s,t,\rho) \in \overline{\Omega} \times [0,T] \times \mathbb{R}$, and

$$|a_{i,j}(s,t,r) - a_{i,j}(s,t,\rho)| \leq K|r-\rho|$$

for all $(s,t,r),(s,t,\rho) \in \overline{\Omega} \times [0,T] \times \mathbb{R}$, $1 \leq i,j \leq d$.

A2 We assume that the matrix $A(s,t,z) \equiv [a_{i,j}(s,t,z)]_{i,j=1}^{d}$ is symmetric, positive definite, and has a spectrum that is bounded above and below by positive constants η_1 and η_2, uniformly so for $(s,t,z) \in \overline{\Omega} \times [0,T] \times \mathbb{R}$.

Theorem 2 *(Douglas and Dupont) Assume the functions $a_{i,j}(s,t,z)$ and $f(s,t,z)$ satisfy the conditions **A1**-**A2**. Let u be the solution of (1)-(3) and assume it is continuously differentiable over $\overline{\Omega} \times [0,T]$. Let u_n be the solution of (12)-(15). Then there are positive constants γ and C for which*

$$\begin{aligned} &\|u-u_n\|_{L^2\times L^\infty}^2 + \gamma\|u-u_n\|_{H_0^1\times L^2}^2 \\ &\quad \leq C\left\{\|u_0-u_{0,n}\|_{L^2}^2 + \|u-w\|_{L^2\times L^\infty}^2 \right. \\ &\qquad \left. +\|u-w\|_{H_0^1\times L^2}^2 + \|\tfrac{\partial}{\partial t}(u-w)\|_{L^2\times L^2}^2\right\} \end{aligned} \tag{16}$$

for any w of the form given on the right side of (12).

The norms used in (16) are given by

$$\begin{aligned} \|v\|_{L^2\times L^\infty} &= \sup_{0\leq t\leq T} \|v(\cdot,t)\|_{L^2(\Omega)} \\ \|v\|_{L^2\times L^2} &= \|v\|_{L^2(\Omega\times[0,T])} \\ \|v\|_{H_0^1\times L^2}^2 &= \int_0^T \|v(\cdot,t)\|_{H_0^1(\Omega)}^2\, dt \end{aligned}$$

The assumptions of the theorem imply the assumptions used in [13, Thm. 7.1], and the conclusion follows from the cited paper.

To apply this theorem, we need bounds on the norms given in (16) for $u-w$. To obtain these, we use the following approximation theoretic result that follows from Ragozin [21].

Lemma 3 *Assume that $g(x,t)$, $\partial g(x,t)/\partial t$ are k times continously differentiable with respect to $x \in \overline{\mathbb{B}}_d$, for some $k \geq 0$ and $0 \leq t \leq T$. Further, assume that all such k^{th}-order derivatives satisfy a Hölder condition with exponent $\gamma \in (0,1]$ and with respect to $x \in \overline{\mathbb{B}}_d$,*

$$\begin{aligned} |h(x,t) - h(y,t)| &\leq c_{k,\gamma}(g)|x-y|^\gamma, \\ \left|\frac{\partial h(x,t)}{\partial t} - \frac{\partial h(y,t)}{\partial t}\right| &\leq c_{k,\gamma}(g)|x-y|^\gamma, \end{aligned}$$

uniformly for $x, y \in \overline{\mathbb{B}}_d$ *and* $0 \leq t \leq T$*, where* h *denotes a generic* k^{th}*-order derivative of* g *with respect to* $x \in \overline{\mathbb{B}}_d$*. The quantity* $c_{k,\gamma}(g)$ *is called the Hölder constant. Let* $\{\varphi_1, \ldots, \varphi_N\}$ *denote a basis of* Π_n*. Then for each degree* $n \geq 1$*, there exists*

$$g_n(x,t) = \sum_{k=1}^{N_n} \beta_k(t)\, \varphi_k(x)$$

which satisfies

$$\max_{0\leq t\leq T} \max_{x\in\overline{\mathbb{B}}_d} |g(x,t) - g_n(x,t)| \leq \frac{b_{k,\gamma}}{n^{k+\gamma}} c_{k,\gamma}(g),$$

$$\max_{0\leq t\leq T} \max_{x\in\overline{\mathbb{B}}_d} \left| \frac{\partial g(x,t)}{\partial t} - \frac{\partial g_n(x,t)}{\partial t} \right| \leq \frac{b_{k,\gamma}}{n^{k+\gamma}} c_{k,\gamma}(g),$$

for some constant $b_{k,\gamma} > 0$ *that is independent of* g*.*

Proof. This result can be obtained by a careful examination of the proof of Ragozin [21, Thm. 3.4]. A similar argument for approximation of a parameterized family $g(x,t)$ over the unit sphere $\mathbb{S}^{d-1}$ is given in [9]. The present result over $\mathbb{B}_d$ follows by combining that of [9, §4.2.5] over $\mathbb{S}^d$ with the argument of Ragozin over $\mathbb{B}_d$. ■

Next, we must look at the approximation of the solution $\widetilde{u}(x,t)$ by means of polynomials of the form given on the right side of (12). To do this, we use a trick from [2, (9)-(15)]. Begin with the result that

$$\Delta : \widetilde{\mathcal{X}}_n \xrightarrow[onto]{1-1} \Pi_n. \tag{17}$$

A short proof is given in [4, §2.2]. For any $t \in [0,T]$, consider a function $\widetilde{u}$ which satisfies $\widetilde{u}(x,t) = 0$ for all $x \in \mathbb{S}^{d-1} = \partial\mathbb{B}_d$. Define $g = \Delta_x \widetilde{u}$. Then

$$\widetilde{u}(x,t) = \int_{\mathbb{B}_d} G(x,y)\, g(y,t)\, dy, \qquad x \in \overline{\mathbb{B}}_d,$$

with G the Green's function for the elliptic boundary value problem

$$\begin{aligned} -\Delta v(x) &= g(x), \qquad x \in \mathbb{B}_d, \\ v(x) &= 0, \qquad x \in \mathbb{S}^{d-1}. \end{aligned}$$

For example, in $\mathbb{R}^2$,

$$G(x,y) = \frac{1}{2\pi} \log \frac{|x-y|}{|\mathcal{T}(x) - y|}, \qquad x, y \in \mathbb{B}_2,$$

with $\mathcal{T}(x)$ the inverse of x with respect to the unit circle $\mathbb{S}^1$. Let $g_n(x,t)$ be the polynomial referenced in the preceding Lemma 3, and define

$$\widetilde{w}_n(x,t) = \int_{\mathbb{B}_d} G(x,y)\, g_n(y,t)\, dy, \qquad x \in \overline{\mathbb{B}}_d. \tag{18}$$

From (17), $\widetilde{w}_n(\cdot,t) \in \widetilde{\mathcal{X}}_n$, $0 \leq t \leq T$; and $\widetilde{w}_n$ is an approximation of the original function $\widetilde{u}$.

Lemma 4 *Assume $\widetilde{u}(\cdot,t) \in C^{k,\gamma}\left(\overline{\mathbb{B}}_d\right)$ for $0 \leq t \leq T$, with $k \geq 2$, $0 < \gamma \leq 1$. Then for $n \geq 1$, the function $\widetilde{w}_n(x,t)$ of (18) is of the form*

$$\widetilde{w}_n(x,t) = \sum_{k=1}^{N_n} \alpha_k(t)\,\widetilde{\psi}_k(x) \tag{19}$$

and it satisfies

$$\left\|\widetilde{u}(\cdot,t) - \widetilde{w}_n(\cdot,t)\right\|_{C\left(\overline{\mathbb{B}}_d\right)} \leq \frac{b_{k,\gamma}\alpha_1(G)}{n^{k+\gamma-2}} c_{k,\gamma}(g), \tag{20}$$

$$\left\|\nabla_x\left[\widetilde{u}(\cdot,t) - \widetilde{w}_n(\cdot,t)\right]\right\|_{C\left(\overline{\mathbb{B}}_d\right)} \leq \frac{b_{k,\gamma}\alpha_2(G)}{n^{k+\gamma-2}} c_{k,\gamma}(g), \tag{21}$$

$$\left\|\frac{\partial}{\partial t}\left[\widetilde{u}(\cdot,t) - \widetilde{w}_n(\cdot,t)\right]\right\|_{C\left(\overline{\mathbb{B}}_d\right)} \leq \frac{b_{k,\gamma}\alpha_1(G)}{n^{k+\gamma-2}} c_{k,\gamma}(g) \tag{22}$$

for $0 \leq t \leq T$. The constants α_1 and α_2 are given by

$$\alpha_1(G) = \max_{x \in \overline{\mathbb{B}}_d} \int_{\mathbb{B}_d} |G(x,y)|\, dy,$$
$$\alpha_2(G) = \max_{x \in \overline{\mathbb{B}}_d} \int_{\mathbb{B}_d} |\nabla_x G(x,y)|\, dy,$$

and these are easily shown to be finite. The remaining constants $b_{k,\gamma}$ and $c_{k,\gamma}(g)$ are taken from Lemma 3.

Proof. For the error in approximating $\widetilde{u}$, we have

$$\widetilde{u}(x,t) - \widetilde{w}_n(x,t) = \int_{\mathbb{B}_d} G(x,y)\left[g(y,t) - g_n(y,t)\right] dy,$$
$$\nabla_x\left[\widetilde{u}(\cdot,t) - \widetilde{w}_n(\cdot,t)\right] = \int_{\mathbb{B}_d} \nabla_x G(x,y)\left[g(y,t) - g_n(y,t)\right] dy,$$
$$\frac{\partial}{\partial t}\left[\widetilde{u}(\cdot,t) - \widetilde{w}_n(\cdot,t)\right] = \int_{\mathbb{B}_d} G(x,y)\frac{\partial}{\partial t}\left[g(y,t) - g_n(y,t)\right] dy$$

Thus

$$\left\|\widetilde{u}(\cdot,t) - \widetilde{w}_n(\cdot,t)\right\|_{C\left(\overline{\mathbb{B}}_d\right)} \leq \alpha_1(G)\left\|g(\cdot,t) - g_n(\cdot,t)\right\|_{C\left(\overline{\mathbb{B}}_d\right)}$$

showing (20); and (21) and (22) follow similarly. ∎

These results can be extended to the approximation of $u(\cdot,t)$ over Ω, by the subspace $\mathcal{X}_n$.

Lemma 5 *Assume $u(\cdot,t) \in C^{k,\gamma}\left(\overline{\Omega}\right)$ for $0 \leq t \leq T$, with $k \geq 2$, $0 < \gamma \leq 1$; and assume $\Phi \in C^m\left(\overline{\mathbb{B}}_d\right)$ with $m \geq k+3$. Then for $n \geq 1$ there exists*

$$w_n(s,t) = \sum_{k=1}^{N_n} \alpha_k(t)\,\psi_k(s), \qquad s \in \overline{\Omega}, \quad 0 \leq t \leq T, \tag{23}$$

for which

$$\|u(\cdot,t) - w_n(\cdot,t)\|_{C(\overline{\Omega})} \leq \frac{\omega_1(k,\gamma,u)}{n^{k+\gamma-2}}, \tag{24}$$

$$\|\nabla_x [u(\cdot,t) - w_n(\cdot,t)]\|_{C(\overline{\Omega})} \leq \frac{\omega_2(k,\gamma,u)}{n^{k+\gamma-2}}, \tag{25}$$

$$\left\| \frac{\partial}{\partial t} [u(\cdot,t) - w_n(\cdot,t)] \right\|_{C(\overline{\Omega})} \leq \frac{\omega_3(k,\gamma,u)}{n^{k+\gamma-2}} \tag{26}$$

for $0 \leq t \leq T$.

Proof. Use the transformation $s = \Phi(x)$ to move between functions over Ω and functions over $\mathbb{B}_d$. By means Lemma 1 for the transformation Φ, these results follow immediately from Lemma 4. ■

Combining these results with the Douglas and Dupont Theorem 2 leads to the following convergence result for the Galerkin method (13)-(15).

Theorem 6 *Assume that the solution u of the parabolic problem (1)-(3) satisfies $u(\cdot,t) \in C^{k,\gamma}\left(\overline{\Omega}\right)$ for $0 \leq t \leq T$, with $k \geq 2$, $0 < \gamma \leq 1$. Moreover, assume the transformation $\Phi \in C^m\left(\overline{\mathbb{B}}_d\right)$ with $m \geq k+3$. Then for $n \geq 1$, the solution u_n of (13)-(15) satisfies*

$$\|u - u_n\|^2_{L^2 \times L^\infty},\ \|u - u_n\|^2_{H_0^1 \times L^2} = \mathcal{O}\left(n^{-(k+\gamma-2)}\right).$$

2.3 Further discussion

Our spectral method applies only to regions Ω with a smooth boundary; but some of the ideas extend to piecewise smooth boundaries. For example, with some special regions a transformation Φ can be used to reformulate the problem (1)-(3) to one over a standard region such as a rectangle or cylinder. New spectral methods can then be defined. Regions Ω with a smooth boundary are less common than those with a piecewise smooth boundary, but they certainly occur in fluid mechanics, in electromagnetic and acoustic wave propagation, and in other application areas. For some interesting applications, including a number in which $\partial\Omega$ is assumed to be smooth, see [27, Chaps. 8-15]. The solving of problems over regions Ω with a smooth boundary is the focus of many of the studies in [10], [11], [12], [17], [23], and [24].

Finite element methods are well-suited to regions with a piecewise smooth polyhedral boundary; and they are particularly well-suited to the use of graded meshes, which are often needed with the possibly singular behaviour in u which occurs more naturally when $\partial\Omega$ is polyhedral or only piecewise smooth. When the boundary is curved, however, whether smooth or piecewise smooth, special adaptations known as isoparametric elements are needed; e.g. see [19, §12.1]. In constrast, our transformation of Ω onto $\mathbb{B}_2$ permits smooth curved boundaries of simply-connected regions Ω to be treated easily. A second difference is that the order of convergence of a finite element method is generally of order $\mathcal{O}(h^\tau)$

for some small integer $\tau > 0$, with h the maximum diameter of the elements being using in the grid that discretizes Ω. In contrast, our spectral methods for problems with a smooth solution u are much more rapidly convergent, resulting in much smaller systems of equations that need to be solved for a given desired accuracy. But our spectral methods will not work well for regions with only a piecewise smooth boundary, including regions with polygonal or polyhedral boundaries.

Another possible difficulty with our problem (1)-(3) is that the boundary condition in (2) is too simple. Although it is standard in the theoretical literature for the numerical treatment of (1) to use the homogeneous boundary condition (2), how does one handle a nonzero boundary condition, say

$$u(s,t) = u_b(s,t), \qquad s \in \partial\Omega, \quad 0 < t \leq T? \tag{27}$$

The simplest procedure is to find a smooth (at least twice continuously differentiable) function $U_b(s,t)$, $s \in \Omega$, $0 < t \leq T$, which is an extension of u_b to all of Ω. Then introduce a new unknown function v by means of

$$u = v + U_b.$$

Substitute this into (1) to obtain a new equation for v,

$$\frac{\partial v(s,t)}{\partial t} = \sum_{k,\ell=1}^{d} \frac{\partial}{\partial s_k}\left(a_{k,\ell}(s,t,U_b(s,t)+v(s,t))\frac{\partial v(s,t)}{\partial s_\ell}\right) + f_{new}(s,t,v(s,t)) \tag{28}$$

with a suitably defined new term f_{new}. The function v will satisfy the homogeneous boundary condition (2) and a modified initial condition,

$$v(s,0) = u_0(s) - U_b(s,0), \qquad s \in \Omega. \tag{29}$$

How to obtain $U_b(s,t)$? In some cases there is an obvious extension. For example, if $u_b(s,t)$ is a polynomial in s, then simply use that polynomial to define $U_b(s,t)$. In other cases, however, it may not be obvious. Since we can convert our problem over Ω to an equivalent problem over $\mathbb{B}_d$, we describe another construction for U_b, doing so only for cases in which $u_b(s,t)$ is independent of t, a common situation. We also consider only the planar case, although the method generalizes to regions $\Omega \subseteq \mathbb{R}^d$, $d \geq 2$.

Consider being given a function g on the unit circle S^1 and then extending it to a smooth function G defined over the closed unit disk $\overline{\mathbb{B}}_2$. Given a point $x \in \mathbb{B}_2$, $|x| < 1$, take a straight line through x and have it intersect S^1 at the points

$$P_+(\theta) = x + r_+(\theta)\boldsymbol{\eta},$$
$$P_-(\theta) = x - r_-(\theta)\boldsymbol{\eta}.$$

with

$$\boldsymbol{\eta} = (\cos\theta, \sin\theta), \qquad 0 \leq \theta < \pi.$$

We choose $r_+(\theta)$ and $r_-(\theta)$ to be such that

$$|P_+(\theta)| = |x + r_+(\theta)\boldsymbol{\eta}| = 1, \qquad |P_-(\theta)| = |x - r_-(\theta)\boldsymbol{\eta}| = 1$$

and

$$r_+(\theta) = |x - P_+(\theta)|, \quad r_-(\theta) = |x - P_-(\theta)|.$$

Define

$$g_*(\theta; x) = g(P_+(\theta)) - r_+(\theta)\frac{g(P_+(\theta)) - g(P_-(\theta))}{r_+(\theta) + r_-(\theta)}$$

using linear interpolation along the line L. Here and in the following we always identify the function g on the boundary of the unit disk with a 2π periodic function on the real number line. Then define

$$G(x) = \frac{1}{\pi}\int_0^\pi g_*(\theta; x)\, d\theta,$$

the average of the interpolants $g_*(\theta; x)$. For $Q \in S^1$,

$$\lim_{x \to Q} G(x) = g(Q).$$

For details on the construction of g_* and G, see [6, §3]. Note also that

$$\min_{s \in S^1} g(s) \leq G(x) \leq \max_{s \in S^1} g(s).$$

After constructing G, probably by numerical integration, it can be approximated using a truncation of the expansion of G using a basis of orthonormal polynomials. These ideas are discussed at greater length in [6]. Also, having a polynomial as the function U_b makes easier its differentiation. A further analysis of the properties of this extension G is deferred to a future paper.

3 Implementation issues

Recall the method (12)-(15) and the notation used there. For notation, let

$$\mathsf{a}_N(t) = [\alpha_1(t), \ldots, \alpha_N(t)]^{\mathrm{T}}.$$

The system (13) can be written symbolically as

$$G_n \mathsf{a}_N'(t) = B_n(t, u_n)\,\mathsf{a}_N(t) + \boldsymbol{f}_N(t, u_n), \tag{30}$$

$$G_n = [(\psi_k, \psi_\ell)]_{k,\ell=1}^N, \tag{31}$$

$$(B_n(t, u_n))_{k,\ell} = -\sum_{i,j=1}^d \int_\Omega a_{i,j}(s, t, u_n(s,t)) \frac{\partial \psi_k(s,t)}{\partial s_i}\frac{\partial \psi_\ell(s,t)}{\partial s_j}\, ds, \tag{32}$$

$$\boldsymbol{f}_N(t, u_n)_\ell = (f(\cdot, t, u_n(\cdot, t)), \psi_\ell), \qquad \ell = 1, \ldots, N. \tag{33}$$

For the implementation, we discuss separately the cases of $\Omega \subseteq \mathbb{R}^2$ and $\Omega \subseteq \mathbb{R}^3$. In both cases we must address the following issues

A1. Select a basis $\{\psi_1, \ldots, \psi_N\}$ for $\mathcal{X}_n$.

A2. Discuss the numerical integration of the integrals in (31)-(33).

A3. Approximate the initial value u_0 by some $u_{0,n} \in \mathcal{X}_n$, as suggested in (14).

A4. Discuss the solution of the nonlinear system of differential equations (30).

A5. Evaluate the solution u_n at points of Ω for each given t.

Several of these issues were addressed in the previous papers [2], [5], [7], and we refer to the discussion in those papers for more complete discussions. Below we give a brief introduction to these various problems, enough so as to illustrate in §4 the feasibility of our method and its rapid speed of convergence.

An efficient implementation of our spectral method requires that much more attention be given to these issues. For example, efficient evaluation of the approximation $u_n(s,t)$ requires an efficient means to evaluate orthonormal polynomial expansions. The triple recursion relations of Dunkl and Xu [14, §3.2] lead to fast methods of evaluation, varying greatly with the particular orthonormal basis being used. A discussion of a very efficient algorithm is deferred to a future paper.

3.1 Two dimensions

Let $\Pi_n(\mathbb{B}_2)$ denote the restriction to $\mathbb{B}_2$ of the polynomials over $\mathbb{R}^2$. To construct a basis for the approximation space $\mathcal{X}_n$ of (10), begin by choosing an orthonormal basis $\{\varphi_1, \ldots, \varphi_N\}$ for $\Pi_n(\mathbb{B}_2)$, using the standard inner product for $L^2(\mathbb{B}_2)$. The dimension of $\Pi_n(\mathbb{B}_2)$ is

$$N \equiv N_n = \frac{1}{2}(n+1)(n+2)$$

There are many possible choices of an orthonormal basis, a number of which are enumerated in [14, §2.3.2] and [26, §1.2]. We have chosen one that is particularly convenient for our computations. These are the 'ridge polynomials' introduced by Logan and Shepp [20] for solving an image reconstruction problem. We summarize here the results needed for our work.

Let

$$\mathcal{V}_n = \{P \in \Pi_n(\mathbb{B}_2) : (P,Q) = 0 \quad \forall Q \in \Pi_{n-1}\}$$

the polynomials of degree n that are orthogonal to all elements of $\Pi_{n-1}(\mathbb{B}_2)$. Then the dimension of $\mathcal{V}_n$ is $n+1$; moreover,

$$\Pi_n(\mathbb{B}_2) = \mathcal{V}_0 \oplus \mathcal{V}_1 \oplus \cdots \oplus \mathcal{V}_n \tag{34}$$

It is standard to construct orthonormal bases of each $\mathcal{V}_n$ and to then combine them to form an orthonormal basis of $\Pi_n(\mathbb{B}_2)$ using the latter decomposition. As an orthonormal basis of $\mathcal{V}_n$ we use

$$\widetilde{\varphi}_{n,k}(x) = \frac{1}{\sqrt{\pi}} U_n\left(x_1 \cos(kh) + x_2 \sin(kh)\right), \quad x \in D, \quad h = \frac{\pi}{n+1} \tag{35}$$

for $k = 0, 1, \ldots, n$. The function U_n is the Chebyshev polynomial of the second kind of degree n:

$$U_n(t) = \frac{\sin(n+1)\,\theta}{\sin\theta}, \qquad t = \cos\theta, \quad -1 \le t \le 1, \quad n = 0, 1, \ldots$$

The family $\{\widetilde{\varphi}_{n,k}\}_{k=0}^{n}$ is an orthonormal basis of $\mathcal{V}_n$. As a basis of Π_n, we order $\{\widetilde{\varphi}_{n,k}\}$ lexicographically based on the ordering in (35) and (34):

$$\{\widetilde{\varphi}_\ell\}_{\ell=1}^{N} \equiv \{\widetilde{\varphi}_{0,0},\, \widetilde{\varphi}_{1,0},\, \widetilde{\varphi}_{1,1},\, \widetilde{\varphi}_{2,0},\, \ldots,\, \widetilde{\varphi}_{n,0},\, \ldots, \widetilde{\varphi}_{n,n}\}$$

Returning to (10), we define

$$\widetilde{\psi}_{n,k}(x) = \left(1 - |x|^2\right) \widetilde{\varphi}_{n,k}(x)$$

and the basis $\{\psi_{m,k} : 0 \le k \le m,\ 0 \le m \le n\}$ for $\mathcal{X}_n$ is defined using (10),

$$\psi_{m,k}(s) = \widetilde{\psi}_{n,k}(x), \qquad s = \Phi(x).$$

We will also refer to this basis as $\{\psi_1, \ldots, \psi_N\}$. In general, this is not an orthonormal basis; but the hope is that $\{\widetilde{\varphi}_\ell\}_{\ell=1}^{N}$ being orthonormal will result in a reasonably well-conditioned matrix for the linear systems associated with the solution of (13). Examples of this for elliptic problems are given in [2], [5], [7].

To calculate the first order partial derivatives of $\widetilde{\psi}_{n,k}(x)$, we need $U_n'(t)$. The values of $U_n(t)$ and $U_n^{'}(t)$ are evaluated using the standard triple recursion relations

$$\begin{aligned} U_{n+1}(t) &= 2tU_n(t) - U_{n-1}(t) \\ U_{n+1}^{'}(t) &= 2U_n(t) + 2tU_n^{'}(t) - U_{n-1}^{'}(t) \end{aligned}$$

Second derivatives, if needed, can be evaluated similarly.

For the integrals in (13), for any dimension $d \ge 2$, we first transform them to integrals over $\mathbb{B}_d$. For an arbitrary function g defined on Ω, use the transformation $s = \Phi(x)$ to write

$$\int_\Omega g(s)\, ds = \int_{\mathbb{B}_d} g(\Phi(x))\, \det J(x)\, dx$$

with $J(x)$ the Jacobian matrix (7) for $\Phi(x)$. Applying this to the integrals in (13),

$$(\psi_k, \psi_\ell) = \int_\Omega \psi_k(s)\, \psi_\ell(s)\, ds = \int_{\mathbb{B}_d} \widetilde{\psi}_k(x)\, \widetilde{\psi}_\ell(x)\, \det J(x)\, dx \tag{36}$$

$$\begin{aligned} &\left(f\left(\cdot, t, \sum_{k=1}^{N_n} \alpha_k(t)\, \psi_k\right), \psi_\ell\right) \\ &\quad = \int_{\mathbb{B}_d} f\left(\Phi(x), t, \sum_{k=1}^{N_n} \alpha_k(t)\, \widetilde{\psi}_k(x)\right) \widetilde{\psi}_k(x)\, \det J(x)\, dx \end{aligned} \tag{37}$$

$$\sum_{i,j=1}^{d}\int_{\Omega} a_{i,j}\left(s,t,u_n\left(s,t\right)\right)\frac{\partial\psi_k\left(s\right)}{\partial s_i}\frac{\partial\psi_\ell\left(s\right)}{\partial s_j}\,ds$$

$$= \int_{\Omega}\left\{\nabla\psi_k\left(s\right)\right\}^{\mathrm{T}} A\left(s,u_n\left(s,t\right)\right)\left\{\nabla\psi_\ell\left(s\right)\right\}\,ds$$

$$= \int_{\mathbb{B}_d}\left\{\nabla\widetilde{\psi}_k\left(x\right)\right\}^{\mathrm{T}}\widetilde{A}\left(x,t,\sum_{k=1}^{N_n}\alpha_k\left(t\right)\widetilde{\psi}_k\left(x\right)\right)\left\{\nabla\widetilde{\psi}_\ell\left(x\right)\right\}\det J\left(x\right)\,dx \tag{38}$$

with

$$\widetilde{A}\left(x,t,z\right) = J\left(x\right)^{-1} A\left(\Phi\left(x\right),t,z\right) J\left(x\right)^{-\mathrm{T}}. \tag{39}$$

For the numerical approximation of the integrals in (36)-(38) with $d = 2$, the integrals being evaluated over the unit disk $\mathbb{B}_2$, write a general function g as

$$g\left(x\right) = \widehat{g}\left(r,\theta\right) \equiv g\left(r\cos\theta, r\sin\theta\right).$$

Then use the formula

$$\int_{\mathbb{B}_2} g(x)\,dx \approx \sum_{l=0}^{q}\sum_{m=0}^{2q}\widehat{g}\left(r_l,\frac{2\pi\,m}{2q+1}\right)\omega_l\frac{2\pi}{2q+1}r_l \tag{40}$$

with $q \geq 1$ an integer. Here the numbers ω_l are the weights of the $(q+1)$-point Gauss-Legendre quadrature formula on $[0,1]$. The formula (40) uses the trapezoidal rule with $2q+1$ subdivisions for the integration over $\mathbb{B}_2$ in the azimuthal variable. This quadrature (40) is exact for all polynomials $g \in \Pi_{2q}\left(\mathbb{B}_2\right)$.

To approximate the initial condition u_0, as in (14), we approximate $u_0\left(\Phi\left(x\right)\right)$ by its orthogonal projection onto $\widetilde{\mathcal{X}}_n$,

$$\mathcal{P}_n\left(u_0\circ\Phi\right) = \sum_{j=1}^{N_n}\beta_j\widetilde{\psi}_j$$

The coefficients $\{\beta_j\}$ are obtained by solving the linear system

$$\sum_{j=1}^{N_n}\beta_j\left(\widetilde{\psi}_j,\widetilde{\psi}_i\right) = \left(u_0\circ\Phi,\widetilde{\psi}_i\right), \qquad i = 1,\ldots,N_n. \tag{41}$$

We approximate further by applying the numerical integration (40) to each of the inner products in this system. With $q \geq n+2$, the matrix coefficients for the left side of this linear system will be evaluated exactly. The result of solving this system with the associated numerical integration yields an approximation to $u_0\left(\Phi\left(x\right)\right)$; and using $s = \Phi\left(x\right)$, we have an initial estimate of the form given in (14).

To solve the system of ordinary differential equations (13), we have used the MATLAB program `ode15s`, which is based on the multistep BDF methods of orders 1 through 5; see [3, §8.2], [22, p. 60]. In general, there is often

stiffness when solving differential equations that arise from using a method of lines approximation for parabolic problems, and that is our reasoning for using the stiff ode code `ode15s` rather than an ordinary Runge-Kutta or multistep code. No difficulty arose in solving any of our examples when using this code, although further work is needed to know whether or not a stiff ode code is indeed needed. In our numerical examples, we will give some data on condition numbers that arise in our method.

3.2 Three dimensions

Here we denote by $\Pi_n(\mathbb{B}_3)$ the restriction to $\mathbb{B}_3$ of polynomials over $\mathbb{R}^3$ of degree n or less. The first difference to the two dimensional case is that the dimension of $\Pi_n(\mathbb{B}_3)$ is given by

$$N \equiv N_n = \frac{1}{6}(n+1)(n+2)(n+3).$$

But as with the two dimensional case, there is a wide range of orthonormal basis functions; see [14]. We choose the following orthormal basis for $\Pi_n(\mathbb{B}_3)$

$$\begin{aligned}\widetilde{\varphi}_{m,j,k}(x) &= c_{m,j}\, p_j^{(0,m-2j+\frac{1}{2})}(2|x|^2-1) S_{\beta,m-2j}(x) \\ &= c_{m,j}\, |x|^{m-2j}\, p_j^{(0,m-2j+\frac{1}{2})}(2|x|^2-1) S_{\beta,m-2j}\left(\frac{x}{|x|}\right) \qquad (42) \\ & j=0,\ldots,\lfloor m/2\rfloor,\ \beta=0,1,\ldots,2(m-2j),\ m=0,\ldots,n\end{aligned}$$

The constants $c_{m,j} = 2^{\frac{5}{4}+\frac{m}{2}-j}$ normalize the functions to length one. The functions $p^{(0,m-2j+\frac{1}{2})}$ are the normalized Jacobi polynomials on the interval $[-1,1]$ with respect to the inner product

$$(v,w) = \int_{-1}^{1} (1+t)^{m-2j+\frac{1}{2}}\, v(t) w(t)\, dt$$

Finally the functions $S_{\beta,m-2j}$ are spherical harmonic functions given by

$$S_{\beta,k}(\phi,\theta) = \widetilde{c}_{\beta,k} \begin{cases} \cos\left(\frac{\beta}{2}\phi\right) T_k^{\frac{\beta}{2}}(\cos\theta), & \beta \text{ even}, \\ \sin\left(\frac{\beta+1}{2}\phi\right) T_k^{\frac{\beta+1}{2}}(\cos\theta), & \beta \text{ odd} \end{cases}$$

Here the constant $\widetilde{c}_{\beta,k}$ is chosen in such a way that the functions are orthonormal on the unit sphere S^2 in $\mathbb{R}^3$,

$$\int_{S^2} S_{\beta,k}(x) S_{\widetilde{\beta},\widetilde{k}}(x)\, dx = \delta_{\beta,\widetilde{\beta}}\, \delta_{k,\widetilde{k}}.$$

The functions T_k^l are the associated Legendre polynomials; see [18]. In [15], [29], one can also find recurrence formulas for the numerical evaluation of Jacobi and Legendre polynomials and their derivatives.

The bases for the spaces $\widetilde{\mathcal{X}}_n$ and $\mathcal{X}_n$ defined in (9) and (10) are again, see (9) and (10), defined by

$$\widetilde{\psi}_{m,j,k}(x) = \left(1 - |x|^2\right) \widetilde{\varphi}_{m,j,k}(x) \tag{43}$$

$$\psi_{m,j,k}(s) = \widetilde{\psi}_{m,j,k}(x), \qquad s = \Phi(x) \tag{44}$$

For the numerical implementation we can also order the bases in lexicographical order (still using the notation $\widetilde{\psi}$ and ψ), so in the following we can assume that we have bases $\{\widetilde{\psi}_l \mid l = 1, \ldots, N_n\}$ and $\{\psi_l \mid l = 1, \ldots, N_n\}$ of $\widetilde{\mathcal{X}}_n$ and $\mathcal{X}_n$. All integrals which arise in the formulas (30)–(33) for the approximate solution of (13) are transformed to $\mathbb{B}_3$ as has been done in (36)–(38). To evaluate the resulting integrals over the unit ball in $\mathbb{R}^3$ we use spherical coordinates, and a quadrature formula Q_q

$$\begin{aligned}\int_{\mathbb{B}_3} g(x)\,dx &= \int_0^1 \int_0^{2\pi} \int_0^{\pi} \widetilde{g}(r,\theta,\phi) r^2 \sin(\phi) d\phi\, d\theta\, dr \\ &\approx Q_q[\widetilde{g}], \quad \text{where} \\ Q_q[\widetilde{g}] &\equiv \sum_{i=1}^{2q} \sum_{j=1}^{q} \sum_{k=1}^{q} \frac{\pi}{q} \omega_j \nu_k \widetilde{g}\left(\frac{\zeta_k + 1}{2}, \frac{\pi}{2q} i, \arccos(\xi_j)\right)\end{aligned}$$

Here $\widetilde{g}$ is the representation of g in spherical coordinates. The quadrature formula Q_q uses a trapezoidal rule in the θ direction and weighted Gauss–Legendre quadrature formulas in the ϕ (weights ω_j and nodes $\arccos(\xi_j)$) and r direction (weights ν_k and nodes $(\xi_k + 1)/2$), as described in [5]. With the help of this quadrature formula we can also define the numerical approximation of u_0, see (14) and (15), by formula (41).

4 Numerical examples

We begin with planar examples, followed by some problems on regions Ω in $\mathbb{R}^3$. The examples will all be for the equation

$$\frac{\partial u(s,t)}{\partial t} = \Delta u(s,t) + f(s,t,u(s,t)), \qquad s \in \Omega, \quad t \geq 0. \tag{45}$$

To help in constructing our examples, we use

$$f(s,t,z) = f_1(s,t,z) + f_2(s,t). \tag{46}$$

We choose various f_1 to explore the effects of changes in the type of nonlinearity; and f_2 is then defined to make the equation (45) valid for any given u,

$$f_2(s,t) = \frac{\partial u(s,t)}{\partial t} - \{\Delta u(s,t) + f_1(s,t,u(s,t))\}, \; s \in \Omega, \quad t \geq 0. \tag{47}$$

In the reformulation (38), $A = I$ and thus

$$\widetilde{A}(x,t,z) = J(x)^{-1} J(x)^{-\mathrm{T}}. \tag{48}$$

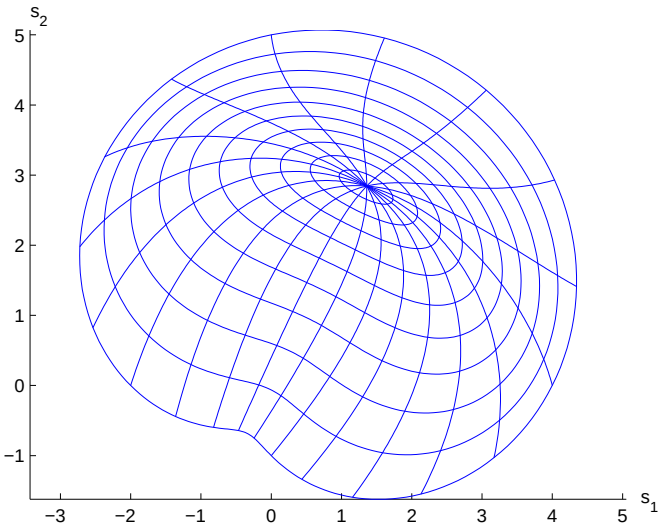

Figure 1: The region Ω associated with (49) and the mapping Φ

4.1 Planar examples

Begin with the region Ω whose boundary is a limacon. In particular, consider the boundary

$$\begin{aligned} &\varphi(\theta) = \rho(\theta)(\cos\theta, \sin\theta), \\ &\rho(\theta) = 3 + \cos\theta + 2\sin\theta, \qquad 0 \le \theta \le 2\pi. \end{aligned} \tag{49}$$

Using the methods of [6], we obtain a mapping $\Phi : \mathbb{B}_2 \to \Omega$. Each component of Φ is a polynomial of degree 3. To illustrate the mapping we show the images in Ω of uniformly spaced circles and radial lines in $\mathbb{B}_2$; see Figure 1 and note that Ω is almost convex.

As a particular example for solving (45), let

$$f_1(s,t,z) = e^{-z}\cos(\pi t), \tag{50}$$

$$u(s,t) = \left(1 - x_1^2 - x_2^2\right)\cos(t + 0.05\pi s_1 s_2) \tag{51}$$

with $s = \Phi(x)$. For the numerical integration in (40), $q = 2n$ was chosen, where $n+2$ is the degree of the approximation $\widetilde{u}_n$. This choice of q has always been more than adequate, and a smaller choice would often have sufficed.

To have a time interval of reasonable length, the problem was solved over $0 \le t \le 20$, although something longer could have been chosen as well. The error was checked at 801 points of Ω, chosen as the images under Φ of 801 points distributed over $\mathbb{B}_2$. The graph of $u_{12}(\cdot, 20)$ is given in Figure 2, and the associated error is given in Figure 3; in addition, $\|u(\cdot,20) - u_{12}(\cdot,20)\|_\infty \doteq$

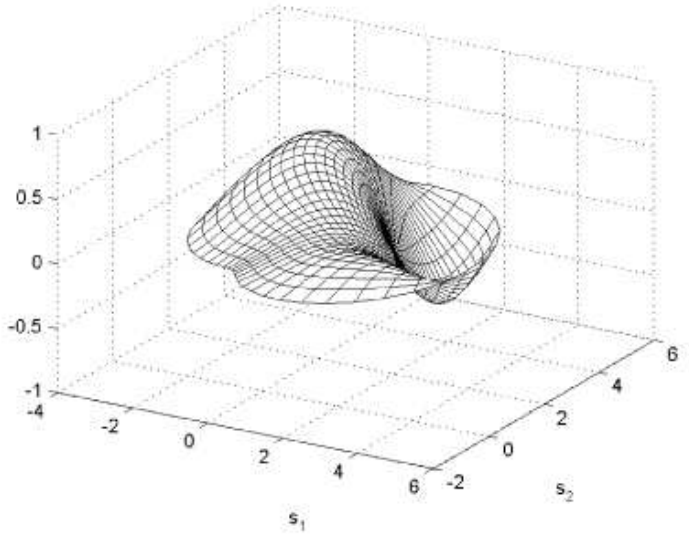

Figure 2: The approximating solution $u_{12}(s, 20)$ for the true solution $u(s, 20)$ of (51) over Ω

$1.94E-4$. Figure 4 shows the error norm $\|u(\cdot,t) - u_{12}(\cdot,t)\|_\infty$ for 200 evenly spaced values of t in $[0, 20]$. There is an oscillatory behaviour which is in keeping with that of the solution u. To illustrate the spectral rate of convergence of the method, Figure 5 gives the error as the degree n varies from 6 to 20. The linear behaviour of this semi-log graph implies an exponential rate of convergence of u_n to u as a function of n.

An important aspect on which we have not yet commented is the conditioning of the matrices in the system (30). In our use of the MATLAB program `ode15s`, we have written (30) in the form

$$\mathsf{a}_N'(t) = G_n^{-1} B_n(t, u_n)\, \mathsf{a}_N(t) + G_n^{-1} \boldsymbol{f}_N(t, u_n), \tag{52}$$

The matrix $G_n^{-1} B_n(t, u_n)$ is the Jacobian matrix for this system. Investigating experimentally,

$$\operatorname{cond}\left(G_n^{-1} B_n\right) = \mathcal{O}\left(N_n^2\right) \tag{53}$$

where N_n is the number of equations in (52). As support for this assertion, Figure 6 shows the graph of $\log\left(N_n^2\right)$ vs. $\log\left(\operatorname{cond}\left(G_n^{-1} B_n\right)\right)$. There is a clear linear behaviour and the slope is approximately 1, thus supporting (53). When Ω is the unit disk, and $\Phi = I$, the result (53) is still valid experimentally.

As a second example, one for which Ω is much more nonconvex (although still star-like), consider the region Ω with the given boundary function

$$\begin{aligned} &\varphi(\theta) = \rho(\theta)(\cos\theta, \sin\theta), \\ &\rho(\theta) = 5 + \sin\theta + \sin 3\theta - \cos 5\theta, \qquad 0 \le \theta \le 2\pi. \end{aligned} \tag{54}$$

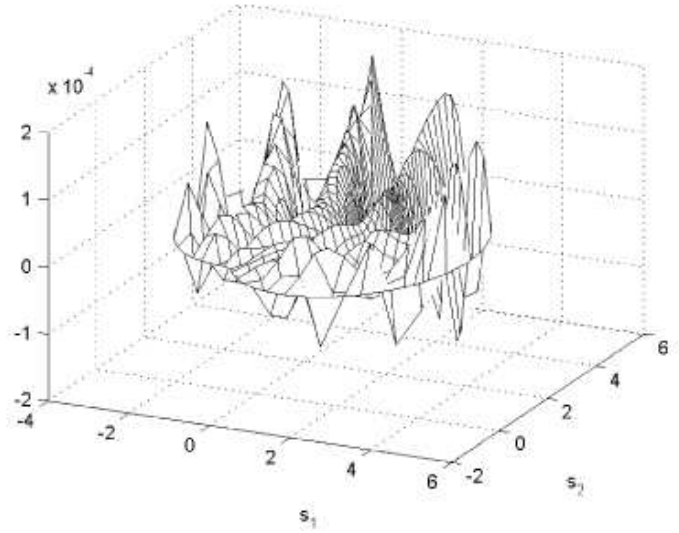

Figure 3: The error in the approximating solution $u_{12}(s, 20)$ for the true solution $u(s, 20)$ of (51) over Ω

As before, an extension Φ to $\mathbb{B}_2$ is constructed using the methods of [6]. The mapping Φ is a polynomial of degree 7 in each component; and the images in Ω of uniformly spaced circles and radial lines in $\mathbb{B}_2$ are shown in Figure 7.

Again, use the function f_1 of (50) and the solution u of (51). The solution $u_{20}(\cdot, 20)$ is shown in Figure 8 over this new region, and $\|u(\cdot, 20) - u_{20}(\cdot, 20)\|_\infty \doteq 0.00136$. Figure 9 shows the error in $u_{20}(\cdot, t)$ over time, and Figure 10 shows how the error in u_n varies with the degree n. The latter again indicates a spectral order of convergence, although slower than that shown in Figure 5. The condition numbers still satisfy the empirical estimate of (53).

4.2 A three-dimensional example

Here we will study one domain Ω which we investigated already in a previous article for the purpose of analyzing the spectral method for Dirichlet problems; see [2]. The domain has the advantage that the transformation Φ is known throughout $\mathbb{B}_3$ and even the inverse transformation Ψ is known explicitly. The knowledge of Ψ is not necessary for the use of the spectral method but makes the construction of an explicit solution easier. The mapping $\Phi : \overline{\mathbb{B}}_3 \mapsto \overline{\Omega}$, $(s_1, s_2, s_3) = \Phi(x_1, x_2, x_3)$ is given by

$$\begin{aligned} s_1 &= x_1 - x_2 + a x_1^2 \\ s_2 &= x_1 + x_2 \\ s_3 &= 2x_3 + b x_3^2 \end{aligned} \tag{55}$$

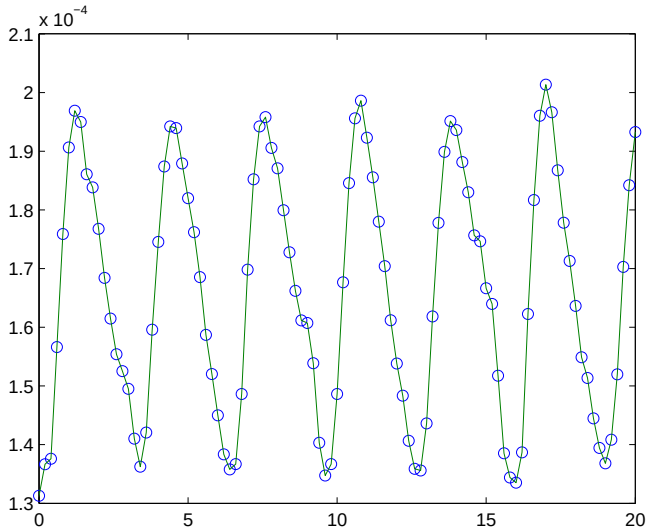

Figure 4: The error $\|u(\cdot,t) - u_{12}(\cdot,t)\|_\infty$ for the true solution $u(s,t)$ of (51)

where $0 < a, b < 1$ are two parameters. Figures 11, 12 show an example of the surface of Ω from two different angles. The inverse $\Psi : \overline{\Omega} \mapsto \overline{\mathbb{B}}_3$ is given by

$$\begin{aligned} x_1 &= \frac{1}{a}\left[-1 + \sqrt{1 + a(s_1 + s_2)}\right] \\ x_2 &= \frac{1}{a}\left[as_2 + 1 - \sqrt{1 + a(s_1 + s_2)}\right] \\ x_3 &= \frac{1}{b}\left[-1 + \sqrt{1 + bs_3}\right] \end{aligned}$$

Furthermore the Jacobian for Φ is given by

$$J(x) = \begin{pmatrix} 1 + 2ax_1 & -1 & 0 \\ 1 & 1 & 0 \\ 0 & 0 & 2 + 2bx_3 \end{pmatrix}$$

with determinant

$$\det(J(x)) = 4(1 + ax_1)(1 + bx_3).$$

This allows us also to calculate $\widetilde{A}$, see (48), directly

$$\widetilde{A}(x) = \begin{pmatrix} \dfrac{1}{2(1+ax_1)^2} & \dfrac{ax_1}{2(1+ax_1)^2} & 0 \\ \dfrac{ax_1}{2(1+ax_1)^2} & \dfrac{1 + ax_1 + 2a^2x_1^2}{2(1+ax_1)^2} & 0 \\ 0 & 0 & \dfrac{1}{4(1+bx_3)^2} \end{pmatrix}$$

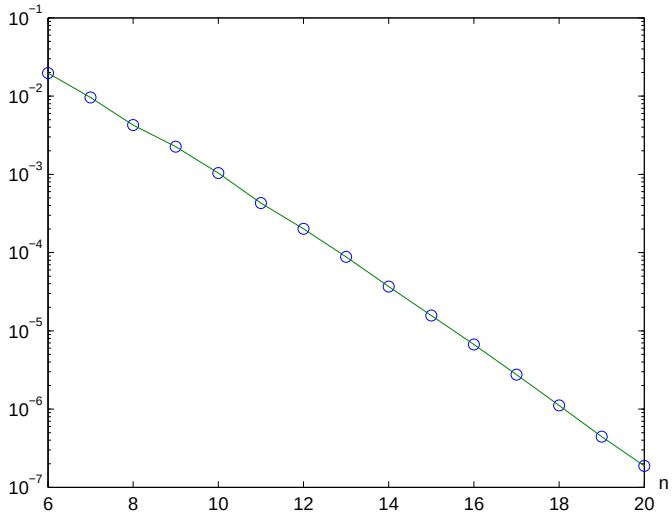

Figure 5: n vs. $\max_{0\le t\le 20} \|u(\cdot,t) - u_n(\cdot,t)\|_\infty$

Again we use the spectral method to solve (45) where f is given by (46) and (47). As a particular example for solving (45), let

$$\begin{aligned} f_1(s,t,z) &= e^{-z}\cos(\pi t), \\ u(s,t) &= (1 - x_1^2 - x_2^2 - x_3^2)\cos(t + 0.05\pi s_1 s_2 s_3) \end{aligned} \tag{56}$$

where $(x_1, x_2, x_3) = \Psi(s_1, s_2, s_3)$ with $a = 0.7$ and $b = 0.9$. Numerical results are given in Figures 13, 14. Figure 15 seems to indicate that the relation (53) for the condition number of the Jacobian $G_n^{-1}B_n$ is also valid in the three dimensional case.

References

[1] M. Abramowitz, I.A. Stegun. *Handbook of Mathematical Functions*, Dover Publications, Inc., New York, 1965.

[2] K. Atkinson, D. Chien, and O. Hansen. A spectral method for elliptic equations: The Dirichlet problem, *Advances in Computational Mathematics,* **33** (2010), pp. 169-189.

[3] K. Atkinson, W. Han, and D. Stewart. *Numerical Solution of Ordinary Differential Equations*, John Wiley Pub., 2009.

[4] K. Atkinson and O. Hansen. Solving the nonlinear Poisson equation on the unit disk, *J. Integral Eqns. & Applic.* **17** (2005), pp. 223-241.

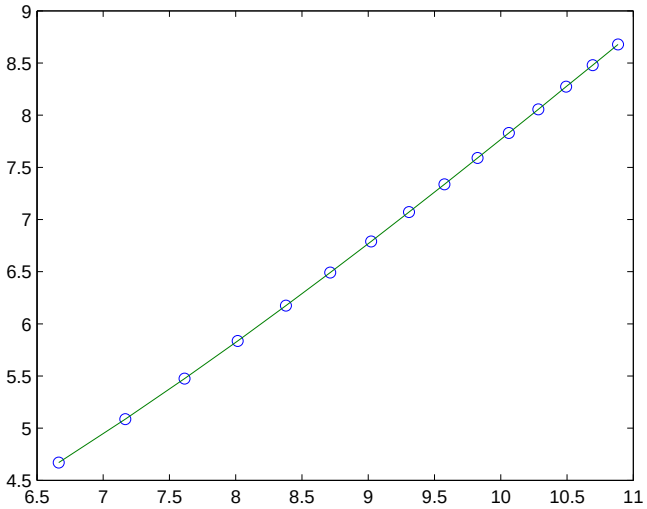

Figure 6: $\log\left(N_n^2\right)$ vs. $\log\left(\text{cond}\left(G_n^{-1}B_n\right)\right)$ for limacon region

[5] K. Atkinson and O. Hansen. A spectral method for the eigenvalue problem for elliptic equations, *Electronic Transactions on Numerical Analysis* **37** (2010), pp. 386-412.

[6] K. Atkinson and O. Hansen. Creating domain mappings, *Electronic Transactions on Numerical Analysis* **39** (2012), pp. 202-230.

[7] K. Atkinson, O. Hansen, and D. Chien. A spectral method for elliptic equations: The Neumann problem, *Advances in Computational Mathematics* **34** (2011), pp. 295-317.

[8] K. Atkinson and W. Han. *Theoretical Numerical Analysis: A Functional Analysis Framework*, 3rd ed., Springer-Verlag, New York, 2009.

[9] K. Atkinson and W. Han. *An Introduction to Spherical Harmonics and Approximations on the Unit Sphere*, Springer-Verlag, New York, 2012.

[10] J. Boyd. *Chebyshev and Fourier Spectral Methods*, 2nd ed., Dover Pub., New York, 2000.

[11] C. Canuto, A. Quarteroni, My. Hussaini, and T. Zang. *Spectral Methods in Fluid Mechanics*, Springer-Verlag, 1988.

[12] C. Canuto, A. Quarteroni, My. Hussaini, and T. Zang. *Spectral Methods - Fundamentals in Single Domains*, Springer-Verlag, 2006.

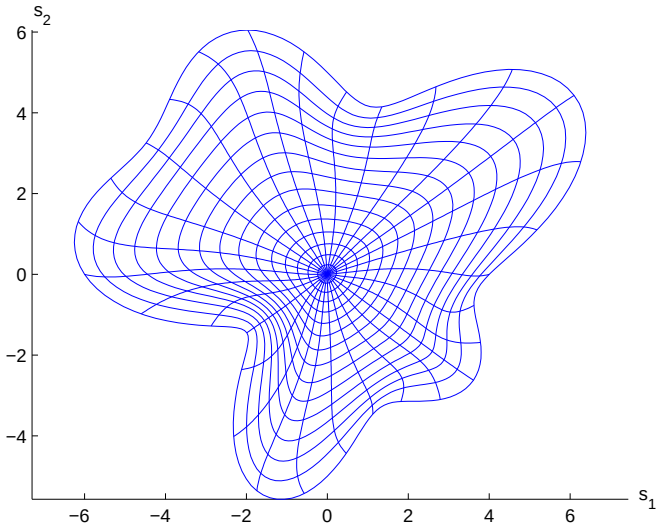

Figure 7: The region Ω associated with (54) and the mapping Φ

[13] J. Douglas and T. Dupont. Galerkin methods for parabolic equations, *SIAM J. Num. Anal.* **7** (1970), 575-626.

[14] C. Dunkl and Y. Xu. *Orthogonal Polynomials of Several Variables*, Cambridge Univ. Press, Cambridge, 2001.

[15] W. Gautschi. *Orthogonal Polynomials*, Oxford University Press, Oxford, 2004.

[16] D. Gottlieb and S. Orszag. *Numerical Analysis of Spectral Methods: Theory and Applications*, SIAM Pub., 1977.

[17] Ben-Yu Guo. *Spectral Methods and Their Applications*, World Scientific, 1998.

[18] E. W. Hobson. *The Theory of Spherical and Ellipsoidal Harmonics*, Chelsea Publishing, New York, 1965.

[19] C. Johnson. *Numerical Solution of Partial Differential Equations by the Finite Element Method*, Cambridge University Press, 1987.

[20] B. Logan and L. Shepp. Optimal reconstruction of a function from its projections, *Duke Mathematical Journal* **42**, (1975), 645–659.

[21] D. Ragozin. Constructive polynomial approximation on spheres and projective spaces, *Trans. Amer. Math. Soc.* **162** (1971), 157-170.

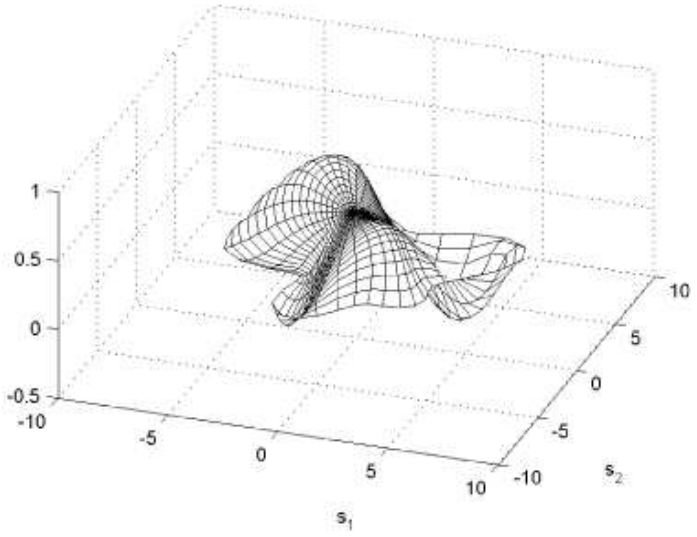

Figure 8: The approximating solution $u_{20}(s, 20)$ for the true solution $u(s, 20)$ of (51) over the Ω of Figure 7

[22] L. Shampine, I. Gladwell, and S. Thompson. *Solving ODEs with MATLAB*, Cambridge University Press, 2003.

[23] J. Shen and T. Tang. *Spectral and High-Order Methods with Applications*, Science Press, Beijing, 2006.

[24] J. Shen, T. Tang, and L. Wang. *Spectral Methods: Algorithms, Analysis and Applications*, Springer-Verlag, 2011.

[25] A. Stroud. *Approximate Calculation of Multiple Integrals,* Prentice-Hall, Inc., Englewood Cliffs, N.J., 1971.

[26] Yuan Xu. Lecture notes on orthogonal polynomials of several variables, in *Advances in the Theory of Special Functions and Orthogonal Polynomials*, Nova Science Publishers, 2004, 135-188.

[27] A. Yagi. *Abstract Parabolic Evolution Equations and Their Applications*, Springer-Verlag, 2010.

[28] E. Zeidler. *Nonlinear Functional Analysis and Its Applications: II/B*, Springer-Verlag, Berlin, 1990.

[29] S. Zhang and J. Jin. *Computation of Special Functions*, John Wiley & Sons, New York, 1996.

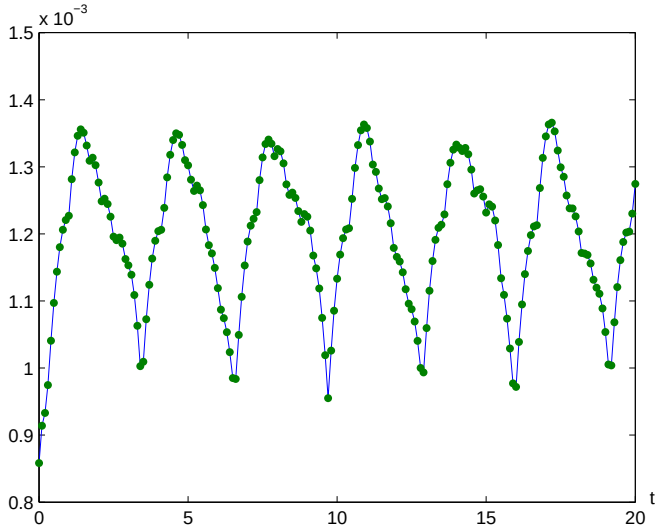

Figure 9: The error $\|u(\cdot,t) - u_{20}(\cdot,t)\|_\infty$ for the true solution $u(s,t)$ of (51) over the Ω of Figure 7

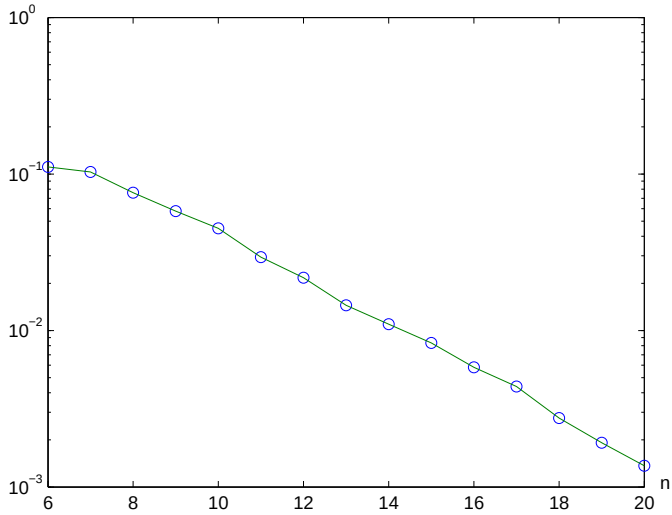

Figure 10: n vs. $\max\limits_{0\le t\le 20} \|u(\cdot,t) - u_n(\cdot,t)\|_\infty$ for the Ω of Figure 7

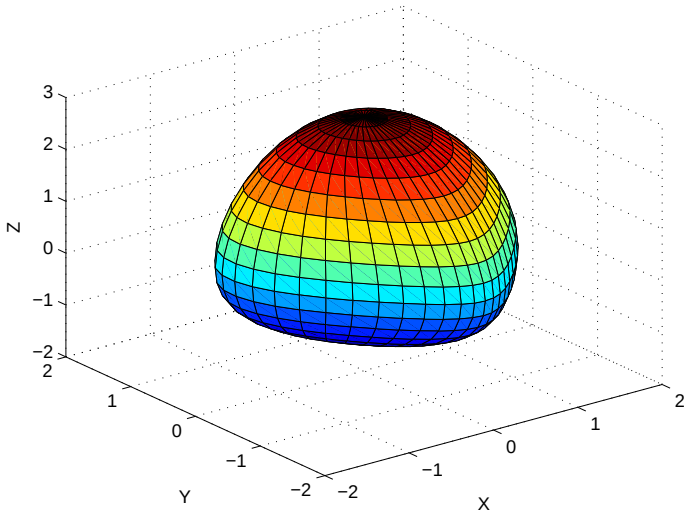

Figure 11: The surface of Ω with parameters $a = 0.7$ and $b = 0.9$; see (55)

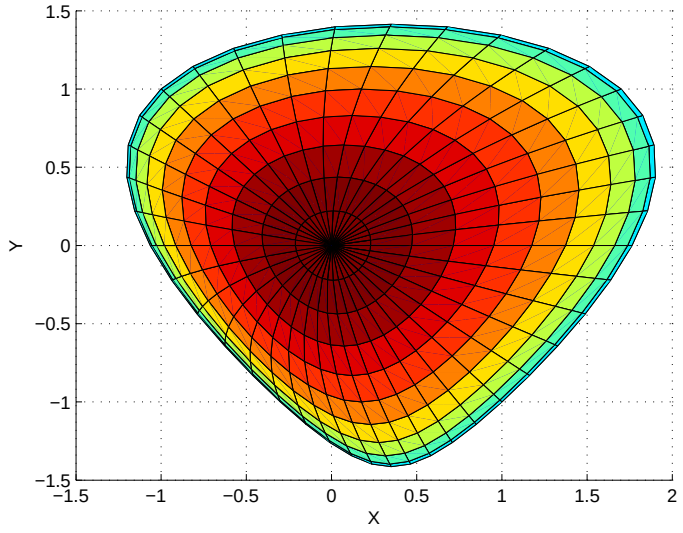

Figure 12: The surface of Ω, see (55), seen from the z-axis

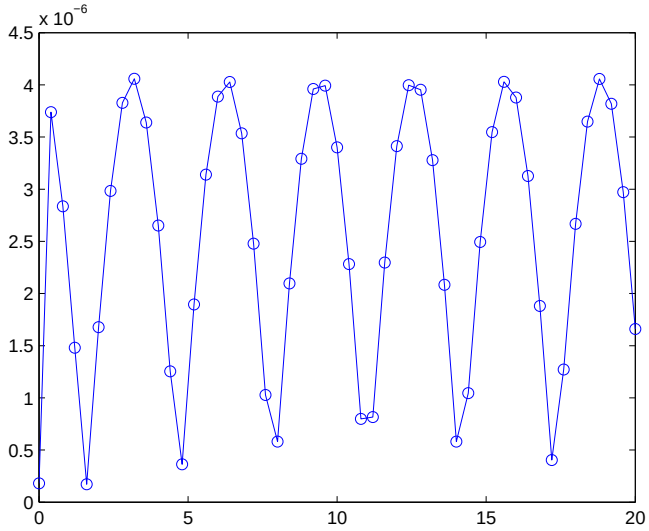

Figure 13: The error $\|u(\cdot,t) - u_{12}(\cdot,t)\|_\infty$ for the true solution $u(s,t)$ of (56) over the Ω of Figure 11

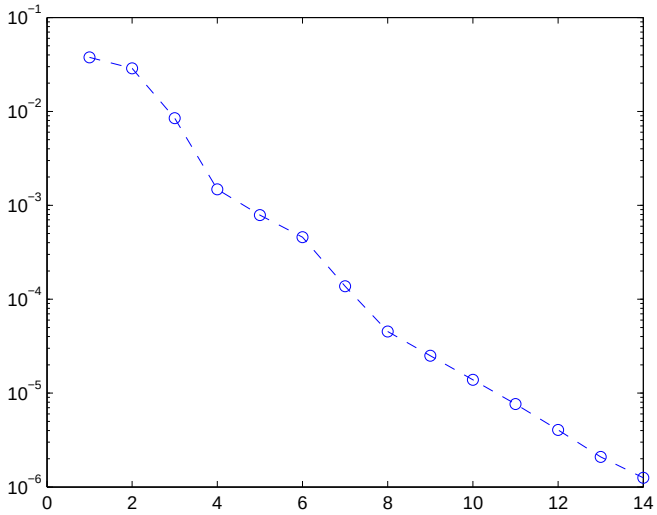

Figure 14: n vs. $\max\limits_{0\le t\le 20} \|u(\cdot,t) - u_n(\cdot,t)\|_\infty$ over the Ω of Figure 11

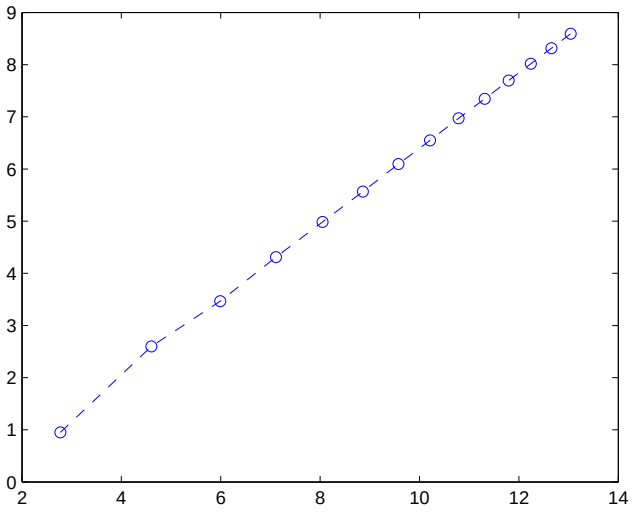

Figure 15: $\log\left(N_n^2\right)$ vs. $\log\left(\text{cond}\left(G_n^{-1}B_n\right)\right)$ for the Ω of Figure 11